Mechanistic Studies on the Reversible Binding of Nitric Oxide to Metmyoglobin

Leroy E. Laverman,[†] Alicja Wanat,[‡,§] Janusz Oszajca,[‡] Grazyna Stochel,*[,‡] Peter C. Ford,*[,†] and Rudi van Eldik*[,§]

Contribution from the Department of Chemistry and Biochemistry, University of California, Santa Barbara, California 93106, Department of Inorganic Chemistry, Jagiellonian University, Ingardena 3, 30-060 Kraków, Poland, and Institute for Inorganic Chemistry, University of Erlangen-Nürnberg, Egerlandstrasse 1, 91058 Erlangen, Germany

Received May 16, 2000. Revised Manuscript Received October 24, 2000

Abstract: The ferriheme protein metmyoglobin (metMb) in buffer solution at physiological pH 7.4 reversibly binds the biomessenger molecule nitric oxide to yield the nitrosyl adduct (metMb(NO)). The kinetics of the association and dissociation processes were investigated by both laser flash photolysis and stopped-flow kinetics techniques at ambient and high pressure, in three laboratories using several different sources of metMb. The activation parameters $\Delta H^{\ddagger}$, $\Delta S^{\ddagger}$, and $\Delta V^{\ddagger}$ were calculated from the kinetic effects of varying temperature and hydrostatic pressure. For the "on" reaction of metMb plus NO, reasonable agreement was found between the various techniques with $\Delta H_{on}^{\ddagger}$, $\Delta S_{on}^{\ddagger}$, and $\Delta V_{on}^{\ddagger}$ determined to have the respective values ~65 kJ mol^{-1}, ~60 J mol^{-1} K^{-1}, and ~20 cm^3 mol^{-1}. The large and positive $\Delta S^{\ddagger}$ and $\Delta V^{\ddagger}$ values are consistent with the operation of a limiting dissociative ligand substitution mechanism whereby dissociation of the H_2O occupying the sixth distal coordination site of metMb must precede formation of the Fe−NO bond. While the activation enthalpies of the "off" reaction displayed reasonable agreement between the various techniques (ranging from 68 to 83 kJ mol^{-1}), poorer agreement was found for the $\Delta S_{off}^{\ddagger}$ values. For this reason, the kinetics for the "off" reaction were determined more directly via NO trapping experiments, which gave the respective activation parameters $\Delta H_{off}^{\ddagger}$ = 76 kJ mol^{-1}, $\Delta S_{off}^{\ddagger}$ = ~41 J mol^{-1} K^{-1}, and $\Delta V_{off}^{\ddagger}$ = 20 cm^3 mol^{-1}), again consistent with a limiting dissociative mechanism. These results are discussed in reference to other investigations of the reactions of NO with both model systems and metalloproteins.

Introduction

Nitric oxide (also known as nitrogen monoxide) has been shown to have important roles in mammalian biology including cytotoxic immune response and intracellular signaling.[1−6] Among the targets for NO modification are the iron centers of certain hemoproteins, and nitrosyl complexes of iron(II) and iron(III) porphyrins are known for functions as diverse as the activation of soluble guanylyl cyclase by nitric oxide[7] to the preservation of meat by sodium nitrite.[8] Under physiological conditions, the formation of such complexes may have importance in the NO inhibition of metalloenzymes such as catalase[9] and cytochrome oxidase,[10] while the release of NO from a salivary ferriheme protein is apparently the key step in vasodilation upon the bite of the blood-sucking insects *Rhodnius prolixus* and *Cimex lecturalis*.[11] Furthermore, nitrosyl iron complexes are likely intermediates if indeed thionitrosyl derivatives of hemoglobin (SNO-Hb) are formed and play a function in blood pressure regulation.[12]

However, despite numerous rate measurements for NO reactions with ferro- and ferriheme centers,[13−19] unanswered

† University of California.
‡ Jagiellonian University.
§ University of Erlangen-Nürnberg.

(1) Ignarro, L. J. A. *Rev. Pharmacol. Toxicol.* **1990**, *30*, 535−560.
(2) Moncada, S. M.; Palmer, R. M.; Higgs, E. A. *Biochem. Pharmacol.* **1989**, *38*, 1709−1713.
(3) Bredt, D. S.; Hwang, P. M.; Glatt, C. E.; Lowenstein, C.; Reed, R. R.; Snyder, S. H. *Nature* **1991**, *351*, 714−718.
(4) Wink, D. A.; Hanbauer, I.; Grisham, M. B.; Laval, F.; Nims, R. W.; Laval, J.; Cook, J.; Pacelli, R.; Liebmann, J.; Krishna, M.; Ford, P. C.; Mitchell, J. B. *Curr. Top. Cell. Regul.* **1996**, *34*, 159−187.
(5) Feelish, M., Stamler, J. S., Eds. *Methods in Nitric Oxide Research*; John Wiley and Sons: Chichester, England, 1996; and references cited therein.
(6) (a) Butler, A. R.; Lyn, D.; Williams, H. *Chem. Soc. Rev.* **1993**, *22*, 233. (b) Williams, R. J. P. *Chem. Soc. Rev.* **1996**, *25*, 77.
(7) (a) Burstyn, J. N.; Yu, A. E.; Dierks, E. A.; Hawkins, B. K.; Dawson, J. H. *Biochemistry* **1995**, *34*, 5896−5903. (b) Kim, S.; Deinum, G.; Gardner, M. T.; Marletta, M. M.; Babcock, G. T. *J. Am. Chem. Soc.* **1996**, *118*, 8769−8770.
(8) Bruun-Jensen, L.; Skibsted, L. H. *Meat Sci.* **1996**, *44*, 145−149.
(9) Brown, G. C. *Eur. J. Biochem.* **1995**, *232*, 188−191.
(10) Cleeter, M. W. J.; Cooper, J. M.; Darley-Usmar, V. M.; Moncada, S.; Scapira, A. H. *FEBS Lett.* **1994**, *345*, 50−54.
(11) (a) Ribeiro, J. M. C.; Hazzard, J. M. H.; Nussenzveig, R. H.; Champagne, D. E.; Walker, F. A. *Science* **1993**, *260*, 539. (b) Valenzuela, J. G.; Walker, F. A.; Ribeiro, J. M. C. *J. Exp. Biol.* **1995**, *198*, 1519. (c) Ding, X. D.; Weichsel, A.; Andersen, J. F. Shokhireva, T. Kh.; Balfour, C.; Pierik, A. J.; Averill, B. A.; Mantfort, W. R.; Walker, F. A. *J. Am. Chem. Soc.* **1999**, *121*, 128−138.
(12) Stamler, J. S.; Jia, L.; Eu, J. P.; McMahon, T. J.; Demchenko, I. T.; Bonaventura, J.; Gernert, K.; Piantadosi, C. A. *Science* **1997**, *276*, 2034−2037.
(13) (a) Gibson, Q. H.; Roughton, F. J. W. *J. Physiol.* **1957**, *136*, 507−526. (b) Fox, J. B.; Thomson, J. S. *Biochemistry* **1963**, *2*, 465−470. (c) Antonini, E.; Brunori, M.; Wyman, J.; Noble, R. *J. Biol. Chem.* **1966**, *241*, 3236−3238. (d) Hoffman, B. M.; Gibson, Q. H. *Proc. Natl. Acad. Sci. U.S.A.* **1978**, *75*, 21−25. (e) Morris, R. J.; Gibson, Q. H. *J. Biol. Chem.* **1980**, *255*, 8050−5053.
(14) Calrson, M. L.; Regen, R.; Elber, E.; Li, H.; Phillips, G. N.; Olson, J. L.; Gibson, Q. H. *Biochemistry* **1994**, *33*, 10597−10606.
(15) Zavarine, I. S.; Kini, A. D.; Morimoto, B. H.; Kubiak, C. P. *J. Phys. Chem. B* **1998**, *102*, 7287−7292.
(16) Kholodenko, Y.; Gooding, E. A.; Dou, Y.; Ikeda-Saito, M.; Hochstrasser, R. M. *Biochemistry* **1999**, *38*, 5918−5924.

10.1021/ja001696z CCC: $20.00
Published on Web 12/15/2000

questions remain concerning the mechanisms by which NO undergoes coordination to metal porphyrin centers (eq 1), especially with regard to reactions with hemoproteins. Clearly,

$$M(Por)_{aq} + NO \underset{k_{off}}{\overset{k_{on}}{\rightleftharpoons}} M(Por)(NO)_{aq} \quad (1)$$

understanding the interaction between nitric oxide and hemoproteins is important for understanding the in vivo chemistry of NO.[20−32] Relevant questions are the following: Since NO is a stable free radical, are the dynamics of its reactions with metal centers dominated by "special" mechanisms owing to this free radical character, or by behavior more typical of normal Lewis base ligands? To what extent is the reaction controlled by the metal−ligand system? Can the results be extended to other metalloproteins and metalloenzymes?

In this context, studies at the University of California, Santa Barbara, were initiated to address temperature and hydrostatic pressure effects for the "on" and "off" reactions with the water-soluble iron(II) and iron(III) porphyrins (M = Fe^{II} or Fe^{III}; Por = TPPS (the tetrakis(4-sulfonatophenyl)porphinato anion) or TMPS (the tetrakis(sulfonatomesityl)porphinato anion) as simplistic models for ferro- and ferriheme proteins.[32,33] From these data, one can extract the activation parameters $\Delta H^{\ddagger}$, $\Delta S^{\ddagger}$, and $\Delta V^{\ddagger}$ to gain insight into the mechanism(s) for the formation and decay of metal nitrosyls. Here attention is turned to the mechanism of the NO reaction with the ferriheme protein metmyoglobin (metMb). Like the iron(III) models, the Fe(III) center of metMb is six coordinate, with a water molecule occupying the site to which NO will coordinate (Figure 1). From a mechanistic perspective, the nitrosyl complex of metmyoglobin is of particular interest, given that both dissociation and association of NO are conveniently observable under physiological temperatures and pH.[20] Indeed, since metmyoglobin reversibly binds nitric oxide, an in vivo NO carrier role for this heme protein might be imagined, given the recent discoveries of NO-carrying ferriheme proteins in insects,[11] as well as proposed schemes with hemoglobin as a NO carrier.[12]

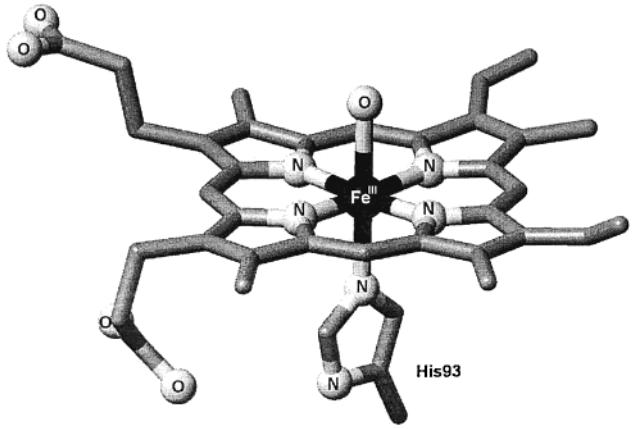

Figure 1. Hexacoordinate iron(III) in the protoporphyrin IX core of aquametmyoglobin as determined by X-ray crystallography. (Kachalova, G. S.; Popov, A. N.; Bartunik, H. D. *Science* **1999**, *284*, 473−476).

The present studies combine the semi-independent results of kinetic investigations of the metMb/NO system by independent laboratories at Santa Barbara, Erlangen, and Krakow. Temperature and (high) hydrostatic pressure effects on the reaction rates were probed by laser flash photolysis and stopped-flow techniques. Here are presented, compared, and discussed detailed kinetic data obtained for the metMb/NO system by the use of these fundamentally different fast kinetics methodologies. Extraction of the appropriate activation parameters provides key insights into the underlying reaction mechanism(s) for the formation and dissociation of the nitrosyl complexes.

Experimental Section

Materials. All solutions were prepared with deionized (Millipore) water. Studies at the University of California, Santa Barbara (UCSB), were performed with equine heart metmyoglobin ($metMb_{(h)}$) purchased from Sigma and equine skeletal muscle metmyoglobin ($metMb_{(s)}$) purchased from CalBioChem, and in most cases the proteins were used as received from the supplier. Gel chromatography (Superdex 200 HR 10/30) of $metMb_{(s)}$ revealed <1% protein impurities, and no experimentally significant differences were noted between kinetic studies performed using proteins as received and those additionally purified by gel chromatography. Tris buffer was prepared from tris(hydroxymethyl)-aminomethane (Aldrich) and Millipore MilliQ filtered and deionized water. The pH was adjusted to 7.0 with HCl and NaOH as needed. Phosphate-buffered saline (PBS, 50 mM, pH 7.4) and phosphate buffer (50 mM, pH 7.0) were purchased from Fluka and Fisher, respectively. Nitric oxide (99.9%) was purchased from Liquid Carbonic and passed through an Ascarite column to remove higher oxides of nitrogen. Salts of $[Ru(HEDTA)Cl]^-$ were prepared according to the method of Diamantis and Dubrawski,[34] and purity was checked by elemental analyses and UV/vis spectroscopy.

Experiments at the Jagiellonian University (JU) and the University of Erlangen-Nürnberg (UEN) were performed using horse skeletal muscle and horse heart myoglobin, purchased from Sigma and purified and converted to metmyoglobin by the following method. A 250 mg sample of the protein was dissolved in 5 mL of 0.1 M Tris buffer solution (pH 7.4) and reduced with sodium dithionite, followed by gel filtration over equilibrated PD-10 columns (Pharmacia; prepacked with Sephadex G-25 medium). The resulting solution was loaded onto an equilibrated column packed with DEAE ion-exchange cellulose (Whatman DE-23). The $metMb_{(s)}$ solution was prepared by addition of a small amount of potassium ferricyanide, $K_3[Fe(CN)_6]$, followed by gel filtration over equilibrated PD-10 column (2−3 times). The collected metmyoglobin fractions were stored at <0 °C. Concentrations were determined spectrophotometrically at 409 nm ($\epsilon = 1.5 \times 10^5$ M^{-1} cm^{-1}). Before each experiment, the metmyoglobin solutions were purged with oxygen-free gas on the vacuum line.

(17) (a) Traylor, T. G.; Magde, D.; Marsters, J.; Jongeward, K.; Wu, G.; Walda, K. *J. Am. Chem. Soc.* **1993**, *115*, 4808−4813. (b) Walda, K. N.; Lieu, X. Y.; Sharma, V. S.; Magde, D. *Biochemistry* **1994**, *33*, 2198−2209.

(18) Chiancone, E.; Elber, R.; Royer, W. E., Jr.; Regan R.; Gibson, Q. H. *J. Biol. Chem.* **1993**, *268*, 5711−5718.

(19) Hoshino, M.; Laverman L. E.; Ford, P. C. *Coord. Chem. Rev.* **1999**, *187*, 75−102.

(20) Hoshino, M.; Ozawa, K.; Seki, M.; Ford, P. C. *J. Am. Chem. Soc.* **1993**, *115*, 9568−9575.

(21) Gordunov, N. V.; Osipov, A. N.; Day, W. B.; Zayas-River, B.; Kagan, V. E.; Elsayed, N. M. *Biochemistry* **1995**, *34*, 6689−6699.

(22) (a) Hoshino, M.; Maeda, M.; Konishi, R.; Seki, H.; Ford, P. C. *J. Am. Chem. Soc.* **1996**, *118*, 5702−5707. (b) Hoshino, M.; Kogure, M. *J. Phys. Chem.* **1989**, *93*, 5478−5484.

(23) Yoshimura, T.; Suzuki, S.; Nakahara, A.; Iwasaki, H.; Masuko, M.; Matsubara, T. *Biochemistry* **1986**, *22*, 3897−3902.

(24) Stochel, G.; Ilkowska, E.; Pawelec M.; Wanat, A.; Wolak, M. *Acta Chim. Hung.—Models Chem.* **1998**, *135*, 847−871.

(25) Morse, R. H.; Chan, S. J. *J. Biol. Chem.* **1980**, *255*, 7876−7882.

(26) Henry, Y.; Banerjee, R. *J. Mol. Biol.* **1973**, 73, 469−482.

(27) Brudvig, G. W.; Stevens, T. H.; Chan, S. J. *Biochemistry* **1980**, *19*, 5275−5285.

(28) Petrich, J. W.; Payat, C.; Martin, J. L. *Biochemistry* **1988**, *27*, 4049.

(29) Antonini, E.; Brunori, M. *Hemoglobin and Myoglobin in Their Reactions with Ligand*; North-Holland Publishing Co.: Amsterdam, 1971.

(30) Duprat, A. F.; Traylor, T. G.; Wu, G.-Z.; Coletta, M.; Sharma, V. S.; Walda, K. N.; Magde, D. *Biochemistry* **1995**, *34*, 2634−2644.

(31) Bohle, D. S.; Hung, Ch.-H. *J. Am. Chem. Soc.* **1995**, *117*, 9584−9585.

(32) Laverman, L. E.; Hoshino, M.; Ford, P. C. *J. Am. Chem. Soc.* **1997**, *119*, 12663−12664.

(33) Laverman, L. E.; Ford, P. C. *Chem. Commun.* **1999**, 1843−1844.

(34) Diamantis, A. A.; Dubrawski, J. V. *Inorg. Chem.* **1981**, *20*, 1142.

Solution Preparation. Solutions used for laser flash photolysis at UCSB were prepared by dissolving protein samples in various buffer solutions and introducing these to a custom-designed cuvette which allows for attachment to a vacuum line. Protein samples were degassed by repeated evacuation of the headspace on a vacuum line with gentle agitation and were equilibrated at a known partial pressure of nitric oxide (P_{NO}) at the desired temperature for a minimum of 20 min. The P_{NO} was measured using a manometer after the equilibration period. NO concentrations were calculated by using reported temperature-dependent mole fraction solubility data.[35] The samples were allowed an additional 10−15 min equilibration time in a temperature-controlled cuvette holder on the flash photolysis instrument. Longer equilibration times did not alter the kinetics behavior. Solutions used for stopped-flow spectroscopy were degassed in an analogous manner in flasks that allowed for the withdrawal of solutions through a three-layer (butyl/silicon/butyl) septum. The NO solutions were equilibrated at 35 °C to prevent bubble formation as the temperature was changed from 15 to 35 °C. Solutions were transferred to the stopped-flow apparatus via a gastight syringe. Aqueous solutions of $[Ru(HEDTA)Cl]^-$ were prepared in pH 7.4 water in the absence of buffer to avoid slow side reactions with the buffer.

Solutions used at JU and UEN were prepared using aqueous 0.1 M Tris buffer (Sigma Chemicals), and the acidity was adjusted by adding HCl (Titrisol Merck) to give a pH of 7.4 ± 0.1. Tris buffer was chosen because its acid dissociation constant is practically pressure independent (up to 200 MPa).[36] Buffered solutions of metMb were degassed on the vacuum line without freezing the solutions to avoid denaturation of the protein. The stock solution of nitric oxide was prepared by degassing of 0.1 M Tris buffer solution (pH 7.4) and then saturating with NO (Linde 93 and Riessner, cleaned from traces of higher nitrogen oxides such as N_2O_3 and NO_2 by passing through an Ascarite II column) via vacuum line techniques. Dilutions of known concentration were prepared from this saturated solution.

Measurements. pH measurements were performed on a Metrohm 623 pH meter with a Sigma glass electrode. The [NO] dissolved in the buffer solutions was measured with the use of an NO electrode (World Precision Instruments isolated nitric oxide meter, model ISO-NO).[37] The UV/vis spectra were recorded in gastight cuvettes on a Shimadzu UV-2100 spectrophotometer equipped with a thermostated cell compartment CPS-260. All the instruments used for kinetic measurements were thermostated to ±0.1 °C.

Laser Flash Photolysis. Laser flash photolysis kinetic studies at UCSB were performed on a "pump−probe" system described previously.[38] The samples placed in a temperature-controlled cuvette holder were pumped using excitation pulses (15 ns) of 355 nm light generated from the third harmonic of a Nd:YAG laser (Continuum NY61). The probe source was a 300 W xenon arc lamp passed through monochromators prior to and again after passing through the sample. Changes in transmitted probe light intensity were monitored by a PMT tube coupled to a digitizing oscilloscope, and data were transferred to a computer for subsequent analysis.

Laser flash photolysis studies at JU were carried out with the use of the LKS.60 Spectrometer from Applied Photophysics for detection and a Nd:YAG laser (SURLITE I-10, Continuum) pump source operating in the third (355 nm) harmonic (100 mJ pulses with ~7 ns pulse widths). Spectral changes at 422 nm were monitored using a 100 W xenon arc lamp, monochromator, and photomultiplier tube PMT-1P22. The absorbance reading was balanced to zero before the flash, and data were recorded on a digital storage oscilloscope, DSO HP 54522A. Gastight quartz cuvettes and a pillbox cell combined with high-pressure equipment[39] were used at ambient and under high pressure (up to 100 MPa), respectively.

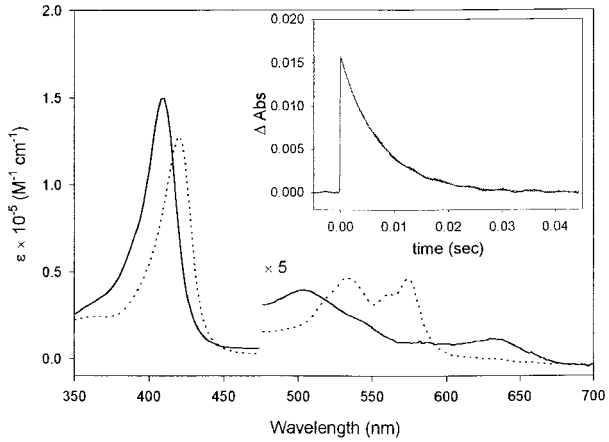

Figure 2. Electronic absorption spectra of $metMb_{(h)}$ (solid line) and $metMb_{(h)}(NO)$ (dotted line) in 50 mM pH 7.4 phosphate buffer solution. Inset: Example of laser flash photolysis kinetic trace at 409 nm for $metMb_{(h)}$ in pH 7.4 PBS, [NO] = 1.8 mM, $k_{obs} = 134\ s^{-1}$.

Stopped-Flow Kinetics. Stopped-flow studies of the NO reaction with $metMb_{(h)}$ at UCSB were carried out using an SX18.MV (Applied Photophysics) stopped-flow spectrometer. Deoxygenated buffered protein solutions were rapidly mixed with solutions at various [NO], and the changes in absorbance at 409 nm were monitored. The experiments conducted at UCSB used a 10:1 (v:v) mixing ratio of NO solution to $metMb_{(h)}$ solution in order to extend the range of [NO] studied.

"Off" rates for dissociation of NO from the nitrosylated protein $metMb_{(s)}(NO)$ were also studied by rapidly mixing $metMb_{(s)}(NO)$ solutions containing a slight excess of NO (~150 μM) with an excess of Na[Ru(HEDTA)Cl] (200 μM) to give $[Ru(HEDTA)NO]^-$ and $metMb_{(s)}$. The reaction was monitored in the stopped-flow spectrometer at 409 and 426 nm, wavelengths where the largest spectral changes were observed.

Stopped-flow studies at JU and UEN were performed by rapidly mixing solutions of $metMb_{(s)}$ and $metMb_{(h)}$ with solutions of NO in 0.1 M Tris buffer at pH 7.4 in stopped-flow spectrometers (SX-17MV and SX-18MV, Applied Photophysics). $K[Ru(HEDTA)Cl]\cdot 2H_2O$ was used as a trapping agent to measure NO dissociation from $metMb_{(s)}$-(NO).

High-Pressure Stopped Flow. High-pressure stopped-flow experiments at UEN were performed on a custom-built instrument described previously[40,41] at pressures up to 130 MPa. Kinetic traces were recorded on an IBM-compatible computer and analyzed with the OLIS KINFIT (Bogart, GA, 1989) set of programs.

All kinetic experiments were performed under pseudo-first-order conditions, i.e., at least a 10-fold excess of nitric oxide. The studied reactions exhibit excellent pseudo-first-order behavior for at least three half-lives. Reported rate constants are the means from at least five kinetic runs, and the quoted uncertainties are based on one standard deviation.

Results

In aqueous solution the optical spectrum of each form of metmyoglobin ($metMb_{(s)}$ and $metMb_{(h)}$) in neutral buffered solution exhibits a Soret band maximum at $\lambda_{max} = 409$ nm ($\epsilon = 1.5 \times 10^5\ M^{-1}\ cm^{-1}$) and a Q-band at 500 nm ($\epsilon = 8.0 \times 10^3\ M^{-1}\ cm^{-1}$). Exposure of a degassed solution of either metMb to excess NO led to spectral shifts giving band maxima at 420 ($\epsilon = 1.3 \times 10^5\ M^{-1}\ cm^{-1}$), 536 ($9.3 \times 10^3$), and 574 nm ($9.4 \times 10^4$) (Figure 2). Upon removal of NO from solution,

(35) Battino, R. In *IUPAC solubility data series, Oxides of Nitrogen*; Young, C. L., Ed.; Pergamon Press: Oxford, 1981; Vol. 8, pp 260−261.
(36) Neuman, R. C., Jr.; Kauzmann, W.; Zipp, A. *J. Phys. Chem.* **1973**, *77*, 2687−2891.
(37) Kudo, S.; Bourassa, J. S. E.; Sato, Y.; Ford, P. C. *Anal. Biochem.* **1997**, *247*, 193.
(38) Lindsay, E.; Ford, P. C. *Inorg. Chim. Acta* **1996**, *242*, 51−56.
(39) Spitzer, M.; Gärtig, F.; van Eldik, R. *Rev. Sci. Instrum.* **1988**, *59*, 2092.
(40) van Eldik, R.; Palmer, D. A.; Schmidt, R.; Kelm, H. *Inorg. Chim. Acta* **1981**, *50*, 131.
(41) van Eldik, R.; Gaede, W.; Wieland, S.; Kraft, J.; Spitzer, M.; Palmer, D. A. *Rev. Sci. Instrum.* **1993**, *64*, 1355.

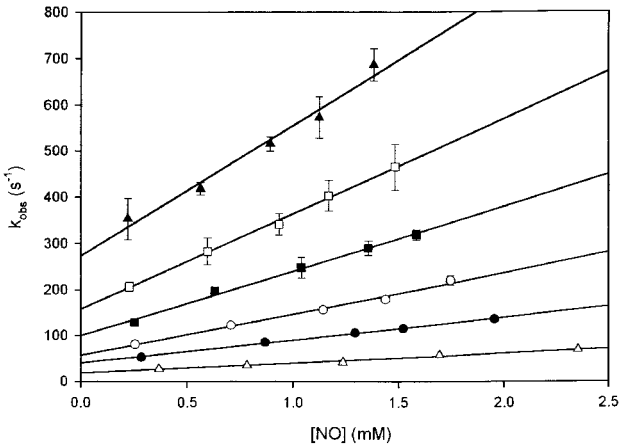

Figure 3. Plot of k_{obs} vs [NO] for the reaction of $metMb_{(h)}$ with NO as measured by laser flash photolysis at different temperatures in pH 7.0 phosphate buffer solution (50 mM): 15 (△), 25 (●), 30 (○), 35 (■), 40 (□), and 45 °C (▲).

the spectral changes were reversed, consistent with the equilibrium described in eq 2. From the spectral changes the

$$\text{metMb}(H_2O) + NO \underset{k_{off}}{\overset{k_{on}}{\rightleftharpoons}} \text{metMb}(NO) + H_2O \qquad (2)$$

equilibrium constant for eq 2 was calculated to be 2.4×10^3 M^{-1} for $metMb_{(s)}$ at 20 °C, pH 7.4 Tris buffer (0.1 M), and this value is consistent with the ratios of the "on" and "off" rate constants ($K = k_{on}/k_{off}$) determined under similar conditions (see below). The K measured here is somewhat smaller than that obtained earlier for sperm whale skeletal muscle metMb in unbuffered pH 6.5 solution (1.3×10^4 M^{-1}), and both values are dramatically smaller than NO binding constants reported for the ferrous forms of myoglobin ($K > 10^{11}$ M^{-1}).[20]

The rate of a reaction such as eq 2, approaching equilibrium with one of the components (in this case NO) in large excess, would be predicted to follow (pseudo) first-order kinetics to give a rate constant k_{obs} which is a function of [NO], i.e.,

$$k_{obs} = k_{on}[NO] + k_{off} \qquad (3)$$

Accordingly, plots of k_{obs} vs [NO] should be linear with slopes equal to k_{on} and nonzero intercepts equal to k_{off}. The rates for Fe(III) porphyrin complexes, including the metmyoglobins, are convenient to measure either by stopped-flow mixing of Fe(III)Por and NO solutions (Figure 3) or by flash photolysis of Fe(III)Por/NO solutions, which displaces the system (Scheme 1) so that relaxation kinetics to equilibrium can be followed by

Scheme 1

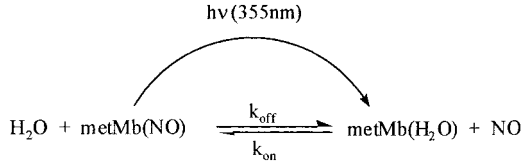

spectrophotometric methods (Figures 2 and 4). Furthermore, the equilibrium constants K are sufficiently small that extrapolation to [NO] = 0 gives a measurable intercept, i.e., k_{off}.

However, such intercepts are susceptible to extrapolation errors. Since the present studies are concerned with measuring the effects of temperature and hydrostatic pressure on these rate constants as functions to determine the activation parameters, accurate values of k_{off} are important. Consequently, the reliability

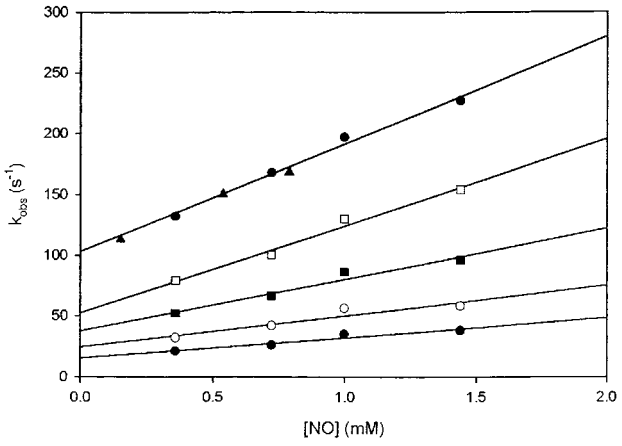

Figure 4. Plot of k_{obs} vs [NO] for the reaction of $metMb_{(h)}$ with NO in pH 7.4 phosphate buffer solution (50 mM) over the temperature range of 15−35 °C as measured by stopped-flow spectroscopy at 15 (●), 20 (○), 25 (■), 30 (□), and 35 °C (▲, ●). (For the data at 35 °C, the two symbols are for two different sources of metMb.)

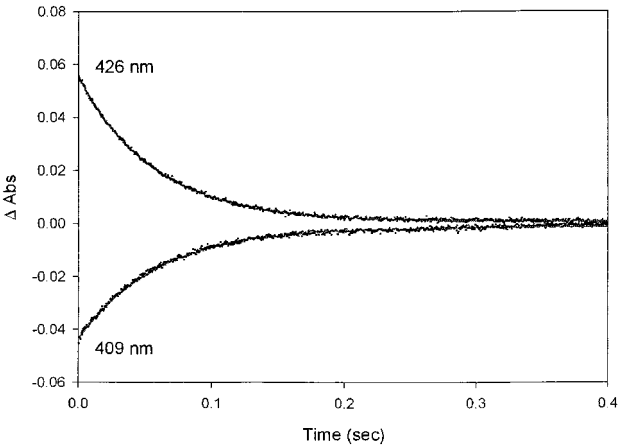

Figure 5. Reaction of metMb(NO) with $[Ru(HEDTA)Cl]^-$ at 20 °C in pH 7.4 phosphate buffer solution (50 mM) monitored at 426 and 409 nm. The two sets of data were fitted to single-exponential functions in each case and gave rate constants of 17 and 18 s^{-1}, respectively.

of k_{off} values obtained from the [NO] dependence of k_{obs} was confirmed more directly by using excess $[Ru(EDTA)H_2O]^-$ as a scavenger for the NO formed by dissociation of metMb(NO), according to Scheme 2. In this experiment, $[Ru(HEDTA)Cl]^-$ rapidly aquates in solution to produce the very labile $[Ru(EDTA)H_2O]^-$ scavenger.

Scheme 2

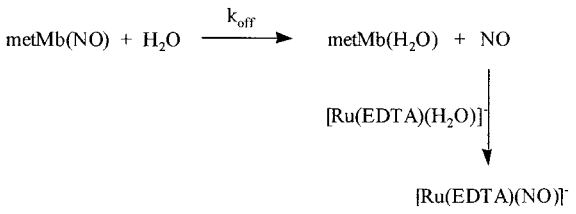

Trapping by $[Ru(EDTA)H_2O]^-$ is sufficiently fast ($k = 2.24 \times 10^7$ M^{-1} s^{-1} in pH 7.4 solution at 7 °C)[42] that, under the conditions chosen, NO release from metMb(NO) is rate limiting ($k_{obs} = k_{off}$) in the reaction sequence depicted by Scheme 2. Figure 5 shows Soret band spectral changes recorded for this reaction, indicating the formation of free metMb. This can be

(42) Davies, N. A.; Wilson, M. T.; Slade, E.; Fricker, S. P.; Murrer, B. A.; Powell, N. A.; Henderson, G. R. *Chem. Commun.* **1997**, 47−48.

Table 1. Rate Constants for the Reaction of NO with metMb(k_{on}) and the NO Dissociation Reaction of metMb(NO) (k_{off}) As Determined by Laser Flash Photolysis

temp (°C)	$k_{on} \times 10^{-4}$ (M^{-1} s^{-1})	k_{off} (s^{-1})
15[a]	2.12 ± 0.2	19 ± 2
25[a]	4.83 ± 0.2	43 ± 3
25[b]	4.80 ± 0.5	42 ± 2
25[c]	4.74 ± 0.3	37 ± 4
25[d]	4.99 ± 0.2	40 ± 2
25[e]	4.88 ± 0.9	56 ± 10
25[f]	6.3 ± 0.4	48 ± 5
30[a]	8.6 ± 0.5	63 ± 6
35[a]	13.2 ± 0.6	113 ± 7
40[a]	19.1 ± 0.7	179 ± 7
45[a]	25.4 ± 0.2	310 ± 20

[a] $metMb_{(h)}$ in 50 mM pH 7.0 phosphate buffer. [b] $metMb_{(h)}$ in 50 mM pH 7.4 phosphate buffer. [c] $metMb_{(h)}$ in 50 mM pH 7.4 Tris. [d] $metMb_{(h)}$ in 50 mM pH 7.4 PBS. [e] $metMb_{(s)}$ in 50 mM pH 7.4 PBS. [f] $metMb_{(s)}$ in 50 mM pH 7.4 PBS, purified by gel chromatography.

measured on the stopped-flow spectrometer time scale, and k_{off} values determined in this manner are independent of the $[Ru(EDTA)H_2O]^-$ concentration and are consistent with, but more accurately determined than, those obtained from extrapolating k_{obs} vs [NO] in the stopped-flow and flash photolysis experiments.

Laser Flash Photolysis Studies. Laser flash photolysis at UCSB of equilibrium $metMb_{(h)}(NO)/metMb_{(h)}$ mixtures in pH 7.0 phosphate buffer under defined P_{NO} gave transient difference spectra consistent with the spectral differences between metMb and metMb(NO), i.e., with labilization of coordinated NO to give nonequilibrium concentrations of these species (Scheme 1). The transient spectra decayed exponentially (inset of Figure 2) to the original spectra, and no permanent photoproducts were observed. The measured values for k_{obs} proved to be independent of observation wavelength. In accord with eq 3, plots of k_{obs} vs [NO] were linear with nonzero intercepts as displayed in Figure 4 for the temperature range 15−45 °C. The k_{on} and k_{off} values determined from these plots (Table 1) were used to construct linear Eyring plots from which were determined the activation parameters $\Delta H^{\ddagger}$ and $\Delta S^{\ddagger}$. The values for k_{on} are $\Delta H^{\ddagger}_{on} = 63 \pm 2$ kJ mol^{-1} and $\Delta S^{\ddagger}_{on} = 55 \pm 8$ J mol^{-1} K^{-1}; for k_{off} these are $\Delta H^{\ddagger}_{off} = 68 \pm 4$ kJ mol^{-1} and $\Delta S^{\ddagger}_{off} = 14 \pm 13$ J mol^{-1} K^{-1}.

Table 1 also summarizes the results of experiments carried out to evaluate possible differences in the kinetics behavior resulting from changes in the medium or metMb source. Flash photolysis experiments with 25 °C solutions of $metMb_{(h)}$ in 50 mM pH 7.0 phosphate buffer, in 50 mM pH 7.4 phosphate buffer, in 50 mM pH 7.4 Tris buffer, and in 50 mM pH 7.4 PBS buffer gave the same values for k_{on} and k_{off} within experimental uncertainties, the uncertainties for k_{off} being larger as expected for values drawn from extrapolations. A limited series of flash photolysis experiments were also carried out in 50 mM pH 7.4 PBS solution using $metMb_{(s)}$ as received from CalBioChem and after gel chromatography. Although there were differences in the k_{on} and k_{off} values somewhat outside experimental uncertainties of the respective $metMb_{(h)}$ experiments, these were not considered significant.

Stopped-Flow Kinetics. Kinetics of the metMb plus NO reaction were examined at UCSB by stopped-flow rapid mixing of PBS solutions (50 mM, pH 7.4) of NO and of deoxygenated $metMb_{(h)}$ and by following the temporal spectral changes. Monitoring the formation of $metMb_{(h)}(NO)$ at 426 nm or disappearance of $metMb_{(h)}$ at 409 nm gave identical k_{obs} values when fit to exponential functions (Figure 3). Plots of k_{obs} vs [NO] were linear with nonzero intercepts over the temperature range of 15−35 °C, consistent with the function $k_{obs} = k_{on}[NO] + k_{off}$ (Table 2). Eyring plots of these data were linear and gave the activation parameters $\Delta H^{\ddagger}_{on} = 63 \pm 4$ kJ mol^{-1} and $\Delta S^{\ddagger}_{on} = 54 \pm 14$ J mol^{-1} K^{-1} and $\Delta H^{\ddagger}_{off} = 65 \pm 5$ kJ mol^{-1} and $\Delta S^{\ddagger}_{off} = 3 \pm 16$ J mol^{-1} K^{-1}, within experimental uncertainties of the respective values measured by flash photolysis (above).

Table 2. Rate Constants for the Forward Binding Reaction of NO with metMb (k_{on}) and the NO Dissociation Reaction of metMb(NO) (k_{off}) As Determined by Stopped Flow

temp (°C)	$k_{on} \times 10^{-4}$ (M^{-1} s^{-1})[a]	k_{off} (s^{-1})[a]	$k_{on} \times 10^{-4}$ (M^{-1} s^{-1})[b]	k_{off} (s^{-1})[b]
10			1.08 ± 0.07	4.5 ± 0.5
15	1.7 ± 0.3	15 ± 3	1.64 ± 0.08	7.8 ± 0.5
20	2.5 ± 0.6	25 ± 6	2.71 ± 0.01	13.4 ± 0.6
25	4.2 ± 0.6	38 ± 6	4.84 ± 0.28	27.6 ± 1.1
30	7.2 ± 0.7	53 ± 6	7.76 ± 0.11	49.2 ± 0.7
35	9.0 ± 0.7	101 ± 6	12.9 ± 0.2	80.8 ± 1.2

[a] Experiments conducted at UCSB with $metMb_{(h)}$ in pH 7.4 phosphate buffer solution. [b] Experiments conducted at JU and UEN with $metMb_{(s)}$ in pH 7.4 Tris buffer solution.

Table 3. Rate Constants for the Dissociation Reaction of MetMb(NO) (k_{off}) As Determined by Trapping Dissociated NO with $[Ru(HEDTA)Cl]^-$

temp (°C)	k_{off}[a] (s^{-1})	k_{off}[b] (s^{-1})
5		2.6 ± 0.3
10	4.8 ± 0.1	5.7 ± 0.5
15	9.0 ± 0.4	9.3 ± 1.5
20	15.5 ± 1.0	16.0 ± 0.4
25	24.2 ± 0.7	28.9 ± 1.4
30	45.4 ± 2.3	49.9 ± 1.8

[a] Values determined at UCSB with $metMb_{(s)}$. [b] Values determined at JU and UEN with $metMb_{(s)}$.

Analogous experiments were performed at JU and UEN using $metMb_{(s)}$ in 0.1 M Tris buffer, and the k_{on} and k_{off} values determined are listed in Table 2 for temperatures ranging from 10 to 35 °C. The respective activation parameters for k_{on} ($\Delta H^{\ddagger}_{on} = 71 \pm 2$ kJ mol^{-1} and $\Delta S^{\ddagger}_{on} = 82 \pm 7$ J mol^{-1} K^{-1}) were in reasonable agreement with those described above, but the temperature dependence of k_{off} gave both a somewhat larger $\Delta H^{\ddagger}_{off}$ (83 ± 2 kJ mol^{-1}) and a larger and more positive $\Delta S^{\ddagger}_{off}$ (62 ± 8 J mol^{-1} K^{-1}).

The range of values reported for $\Delta S^{\ddagger}_{off}$ appears to be in disagreement. However, it should be noted that these data come from stopped-flow experiments in which the k_{off} values are obtained by extrapolation of the k_{obs} vs [NO] plots. Furthermore, the determination of $\Delta S^{\ddagger}$ in principle involves an extrapolation to $1/T = 0$, which leads to differences in the $\Delta S^{\ddagger}$ values between different experiments apparently much larger than indicated by standard deviations for individual experiments. This discrepancy was the motivating factor for measuring the dissociation rates directly using trapping techniques.

NO Labilization from metMb(NO) with Trapping by $[Ru^{III}(EDTA)H_2O]^-$. These kinetic experiments at JU and UEN involved stopped-flow mixing of a $metMb_{(s)}(NO)$ (5 μM) in 0.1 M Tris buffer solution at pH 7.4 with a pH 7.4 aqueous solution of $[Ru(EDTA)(H_2O)]^-$ (500 μM). Spectral changes were monitored at 409 and 421 nm, and the k_{off} values determined at temperatures ranging from 5 to 30 °C are summarized in Table 3. A linear Eyring plot of these data gave the activation parameters $\Delta H^{\ddagger}_{off} = 78 \pm 2$ kJ mol^{-1} and $\Delta S^{\ddagger}_{off} = 46 \pm 7$ J mol^{-1} K^{-1}.

Parallel experiments conducted at UCSB involved stopped-flow mixing of $metMb_{(s)}(NO)$ (7.3 μM) (under a small excess of NO) in pH 7.4 PBS solution with a pH 7.4 aqueous solution

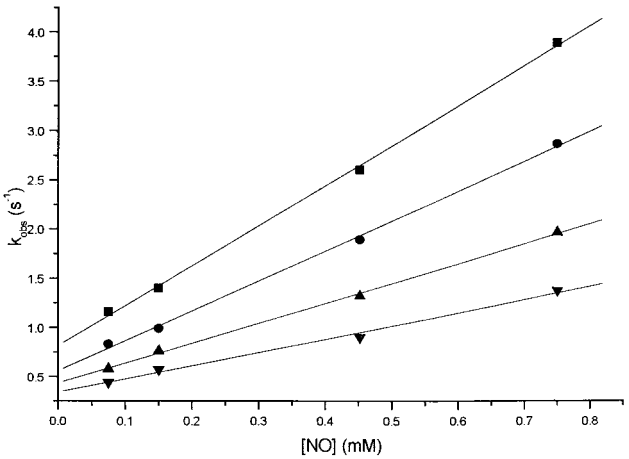

Figure 6. Plot of k_{obs} vs [NO] for the reaction of $metMb_{(s)}$ with NO over the pressure range of 10−130 MPa as measured by stopped-flow spectroscopy at 10 (■), 50 (●), 90 (▲), and 130 MPa (▼). Experimental conditions: [metMb] = 4.2×10^{-6} M, 0.1 M Tris buffer, pH 7.4, temp = 5 °C, λ = 409 nm.

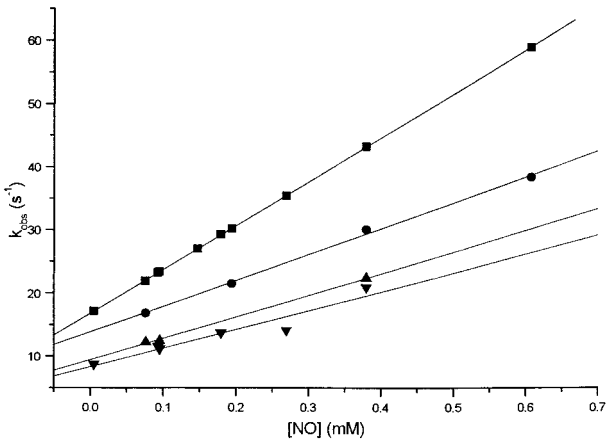

Figure 7. Plot of k_{obs} vs [NO] for the reaction of $metMb_{(s)}$ with NO over the pressure range of 0.1−100 MPa as measured by laser flash photolysis at 0.1 (■), 30 (●), 60 (▲), and 100 MPa (▼). Experimental conditions: [metMb] = 5×10^{-6} M, 0.1 M Tris buffer, pH 7.4, temp = 20 °C, λ = 422 nm.

of $[Ru(HEDTA)Cl]^-$ (200 μM). Spectral changes were monitored at 409 ($metMb_{(s)}$) and 426 nm ($metMb_{(s)}(NO)$) (Figure 5). The k_{off} values reported for 10−30 °C are averages of several acquisitions at each wavelength (Table 3). A linear Eyring plot of these data gave the activation parameters $\Delta H^{\ddagger}_{off}$ = 75 ± 5 kJ mol^{-1} and $\Delta S^{\ddagger}_{off}$ = 36 ± 17 J mol^{-1} K^{-1}, which are in excellent agreement with those found at JU and UEN. Notably, the $\Delta H^{\ddagger}_{off}$ and $\Delta S^{\ddagger}_{off}$ values determined by the two trapping experiments lie between the extremes of the values measured by the extrapolation methods. Given the greater accuracy of the trapping method, the discussion below will focus on the values derived in this manner.

High-Pressure Experiments. Further information on the reaction mechanism comes from the activation volumes ($\Delta V^{\ddagger}_{i} = -RT(\mathrm{d}\ln(k_i)/\mathrm{d}P)_T$, where k_i is the rate constant at a particular P)[43,44] derived from the effect of hydrostatic pressure P on the kinetics. The pressure effect on the reaction of $metMb_{(s)}$ with NO was studied by using two kinetic techniques, viz. stopped-flow mixing (UEN) and flash photolysis (JU). In both cases, the solutions were prepared in Tris buffer at pH 7.4. The stopped-flow experiments were carried out at 5 °C, while the flash photolysis experiments were carried out at 20 °C. The results are reported in Figures 6 and 7, respectively.

From plots of k_{obs} vs [NO] at different P, values of k_{on} and k_{off} were determined, and linear $\ln(k_i)$ vs P plots clearly show that both rate constants decrease with increasing pressure; i.e., both activation volumes are substantially positive (stopped-flow data plotted in Figure 8). The high-pressure stopped-flow experiment gave the values $\Delta V^{\ddagger}_{on}$ = +21.3 ± 0.3 cm^3 mol^{-1} and $\Delta V^{\ddagger}_{off}$ = +16.3 ± 1.3 cm^3 mol^{-1}. The high-pressure flash photolysis experiments gave $\Delta V^{\ddagger}_{on}$ = +19.6 ± 5.7 cm^3 mol^{-1} and $\Delta V^{\ddagger}_{off}$ = +18.5 ± 3.2 cm^3 mol^{-1}, which are equivalent within experimental uncertainties. The larger error limits for the flash photolysis experiment are due to the low quantum yield, ϕ_{dis}, for metMb formation from metMb(NO) in the high-pressure cell, resulting in smaller signal-to-noise ratios. The reaction volume ΔV for the overall equilibrium ($\Delta V = \Delta V^{\ddagger}_{on} - \Delta V^{\ddagger}_{off}$), is small, viz. +5 ± 2 and +1 ± 8 cm^3 mol^{-1} from the stopped-flow and flash photolysis data, respectively. Thus, there is little overall change in the partial molar volume during NO binding to metMb. A volume profile constructed on the basis of the stopped-flow data is illustrated in Figure 9.

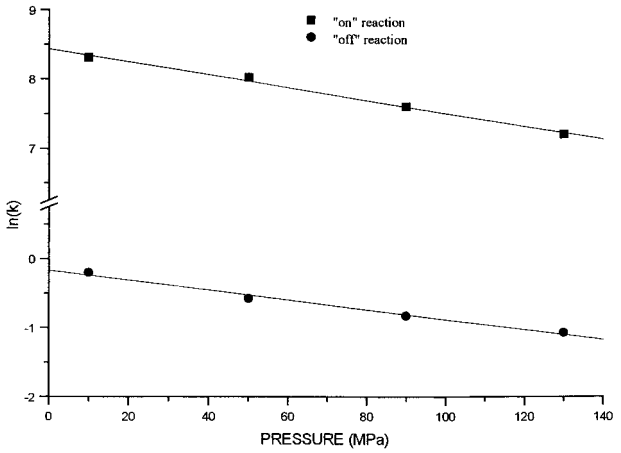

Figure 8. Plots of $\ln(k_{on})$ and $\ln(k_{off})$ versus pressure for the reaction of $metMb_{(s)}$ with NO for the stopped-flow data reported in Figure 6. Experimental conditions: see Figure 6.

The effect of pressure on the NO trapping experiment with $[Ru(edta)H_2O]^-$ was also investigated using stopped-flow techniques, since the ambient pressure kinetics (stopped-flow and flash photolysis) demonstrated that the "off" reaction can be monitored more accurately in this way. The pressure dependence is reported in Figure 10, from which it follows that $\Delta V^{\ddagger}_{off}$ = +20 ± 1 cm^3 mol^{-1}. This value is in close agreement with those obtained in the stopped-flow and flash photolysis experiments described above. Further experiments demonstrated that identical values for $\Delta V^{\ddagger}_{off}$ are obtained independent of the selected wavelength, viz., 409 or 421 nm. A slightly higher value for $\Delta V^{\ddagger}_{off}$ of +23 ± 1 cm^3 mol^{-1} was found at 20 °C, which further supports the dissociative nature of the "off" reaction.

Discussion

Described here are several semi-independent kinetic studies from three laboratories of the temperature and hydrostatic pressure effects on the reaction of metMb with NO at several

(43) (a) Drljaca, A.; Hubbard, C. D.; van Edik, R.; Asano, T.; Basilewsky, M. V.; le Noble, W. J. *Chem. Rev.* **1998**, *98*, 2167. (b) Stochel, G.; van Eldik, R. *Coord. Chem. Rev.* **1999**, *187*, 329.

(44) (a) Crane, D. R.; Ford, P. C. *J. Am. Chem. Soc.* **1991**, *113*, 8510−8516. (b) Traylor, T. G.; Luo, J.; Simon, J. A.; Ford, P. C. *J. Am. Chem. Soc.* **1992**, *114*, 4340−4345.

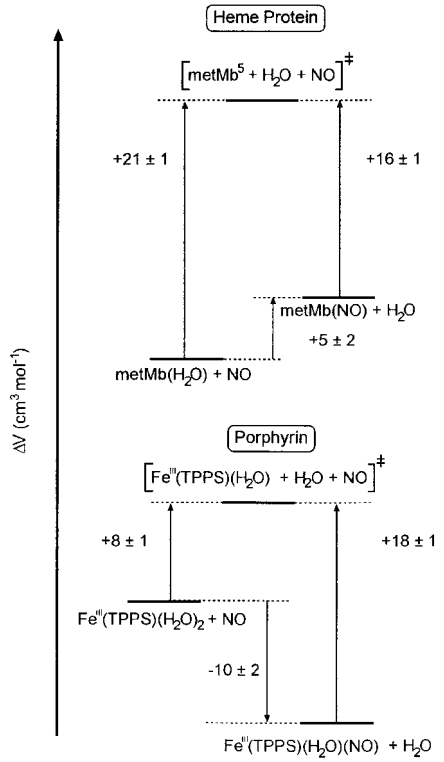

Figure 9. Volume profiles for the reactions. Upper: metMb(H_2O) + NO ⇌ metMb(NO) + H_2O (data from Figure 8). Lower: Fe^{III}(TPPS)-(H_2O)$_2$ + NO ⇌ Fe^{III}(TPPS)(H_2O)(NO) + H_2O (ref 32).

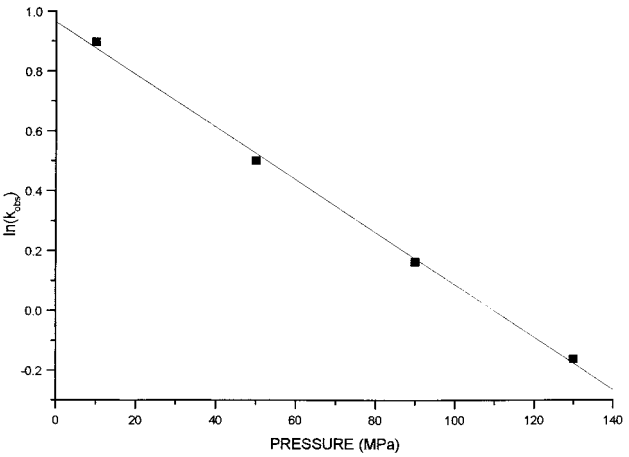

Figure 10. Plot of ln(k_{obs}) vs pressure for the trapping of NO by [Ru(EDTA)H_2O]$^-$ from metMb(NO) according to the reaction outlined in Scheme 2. Experimental conditions: [metMb(NO)] = 4.2×10^{-6} M, [Ru(EDTA)H_2O^-] = 5×10^{-4} M, 0.1 M Tris buffer, pH 7.4, temp = 10.4 °C, λ = 421 nm.

[NO] over a temperature range of 5−45 °C and a pressure range of 0.1−130 MPa. From these data the activation parameters $\Delta H^{\ddagger}$, $\Delta S^{\ddagger}$, and $\Delta V^{\ddagger}$ for the "on" and "off" reactions were obtained by standard methods. These values are summarized in Table 4. The activation parameters for the formation of the nitrosyl metMb complexes (the "on" reaction) show a reasonable agreement between measurements made by the various laboratories, using several methods, conditions, and sources of the protein. The $\Delta H^{\ddagger}_{on}$ values are large, falling into the range 63−71 kJ mol^{-1}, and $\Delta S^{\ddagger}_{on}$ and $\Delta V^{\ddagger}_{on}$ values are large and positive, all features also seen for the "on" reactions of the water-soluble model compounds Fe^{III}(TPPS) and Fe^{III}(TMPS), the respective activation parameter values being 70 and 62 kJ mol^{-1}, +100 and + 86 J mol^{-1} K^{-1}, +8.3 and +13 cm^3 mol^{-1}.[32] The pattern of large and positive $\Delta S^{\ddagger}_{on}$ and, more diagnostically, large and positive $\Delta V^{\ddagger}_{on}$ values represents a signature for a dissociative ligand substitution mechanism, and such a mechanism was proposed in the previous work on model complexes.[32] In agreement with this proposal is the reported rapid exchange between Fe^{III}(TPPS)-coordinated and bulk water molecules (k_{ex} = 1.4×10^7 s^{-1} at 25 °C),[45] and the dissociative nature of this reaction is indicated by the large and positive activation entropy[45] and activation volume for this reaction.[46]

Table 4. Activation Parameters for the Reaction of NO with metMb As Determined by Several Different Methods

	$\Delta H^{\ddagger}$ (kJ mol^{-1})	$\Delta S^{\ddagger}$ (J mol^{-1} K^{-1})	$\Delta V^{\ddagger}$ (cm^3 mol^{-1})
	k_{on}		
laser flash photolysis[a,c]	63 ± 2	55 ± 8	
stopped-flow[a,c]	63 ± 4	54 ± 14	
stopped-flow[b,d,e]	71 ± 2	82 ± 7	21 ± 1[f]
laser flash photolysis[b,d]			20 ± 6[g]
	k_{off}		
laser flash photolysis[a,c]	68 ± 4	14 ± 13	
stopped-flow[a,c]	65 ± 5	3 ± 16	
trapping[b,c]	75 ± 5	36 ± 17	
trapping[b,d,e]	78 ± 2	46 ± 7	20 ± 1[h]
stopped-flow[b,d,e]	83 ± 2	62 ± 8	16 ± 1[f]
laser flash photolysis[b,d]			18 ± 3[g]

[a] Horse heart metmyoglobin, $metMb_{(h)}$. [b] Horse skeletal metmyoglobin, $metMb_{(s)}$. [c] Experiments conducted at UCSB. [d] Experiments conducted at JU and UEN ($\Delta H^{\ddagger}$ and $\Delta S^{\ddagger}$). [e] Experiments conducted at UEN ($\Delta V^{\ddagger}$). [f] Temp = 5 °C. [g] Temp = 20 °C. [h] Temp = 10 °C.

A similar mechanism would seem an appropriate explanation of the activation parameters for the nitrosylation of metMb, i.e.,

$$\text{metMb}(H_2O) \underset{k_{-1}}{\overset{k_1}{\rightleftharpoons}} \text{metMb}^5 + H_2O \qquad (4)$$

$$\text{metMb}^5 \underset{k_{-2}}{\overset{k_2}{\rightleftharpoons}} \text{metMb(NO)} \qquad (5)$$

where $metMb^5$ is the five-coordinate intermediate formed by H_2O dissociation. If the steady-state approximation is made with respect to the intermediate species $metMb^5$, then the expression for the observed first-order relaxation rate becomes

$$k_{obs} = \frac{k_1 k_2[NO] + k_{-1}k_{-2}[H_2O]}{k_{-1}[H_2O] + k_2[NO]} \qquad (6)$$

Under the experimental conditions, it may be assumed that $k_{-1}[H_2O] \gg k_2[NO]$ since both k_{-1} and k_2 involve ligand trapping of an unsaturated metal center and $[H_2O] \gg [NO]$. If so, the expression for the observed rate constant takes the form of $k_{obs} = k_{on}[NO] + k_{off}$, i.e.,

$$k_{obs} = \frac{k_1 k_2[NO]}{k_{-1}[H_2O]} + k_{-2} \qquad (7)$$

where $k_{on} = k_1k_2/k_{-1}[H_2O]$ and $k_{off} = k_{-2}$. The simplified form of the rate law is valid in the absence of a nonlinear dependence of k_{obs} on [NO].

Accordingly, the activation parameters for k_{on} represent the following sums:

(45) Ostrich, I. J.; Liu, G.; Dodgen, H. W.; Hunt, J. P. *Inorg. Chem* **1980**, *19*, 619−621.
(46) Schneppensieper, T.; Zahl, A.; van Eldik, R., submitted for publication.

$$\Delta H^{\ddagger}_{on} = \Delta H^{\ddagger}_{1} + \Delta H^{\ddagger}_{2} - \Delta H^{\ddagger}_{-1} \quad (8)$$

$$\Delta S^{\ddagger}_{on} = \Delta S^{\ddagger}_{1} + \Delta S^{\ddagger}_{2} - \Delta S^{\ddagger}_{-1} \quad (9)$$

$$\Delta V^{\ddagger}_{on} = \Delta V^{\ddagger}_{1} + \Delta V^{\ddagger}_{2} - \Delta V^{\ddagger}_{-1} \quad (10)$$

Since the k_{-1} and k_2 steps both involve ligand reactions with an unsaturated metal center, the difference in their activation parameters, e.g., $\Delta H^{\ddagger}_2 - \Delta H^{\ddagger}_{-1}$, should be small. In this context, the first step, the dissociation of a water ligand to form the unsaturated intermediate, dominates the activation parameters. The k_1 step should display a sizable $\Delta H^{\ddagger}$, indicative of the energy required to break the $Fe^{III}(Por)-OH_2$ bond, a large positive $\Delta S^{\ddagger}$ due to the formation of two species from one without any significant changes in solvation, and a large positive $\Delta V^{\ddagger}$ for similar reasons. This is the behavior seen for the metMb systems examined here as well as for the water-soluble ferriheme models.

For a more detailed interpretation of the reported activation parameters, an important structural aspect of metMb(NO) should be mentioned. It has been shown from FTIR and resonance Raman data that the reaction product metMb(NO) formally has a linear $Fe^{II}-NO^{+}$ character, which means that partial charge transfer from NO to Fe^{III} occurs during the bonding process.[47] This assignment is consistent with the predictions of Enemark and Feltham regarding the structure of diatomic ligands axially bound to metalloporphyrins.[48] Recent multiple scattering XAFS analyses of metMb(NO) confirm this structural assignment.[49]

Notably, the k_{-1} pathway occurs between two high-spin Fe(III) species, so the volume change involves primarily formation of the $Fe^{III}-OH_2$ bond. In contrast, the k_2 pathway involves not only Fe−NO bond formation but considerable charge transfer from NO to give (formally) an $Fe^{II}-NO^{+}$ species and change from a quintet spin state to a diamagnetic complex. For model porphyrin complexes, the high-spin Fe(III) to low-spin Fe(III) transformation is accompanied by a negative contribution to ΔV,[43,50] as is the coordination-induced high-spin to low-spin transformation of Fe(II).[44b] Earlier studies have reported a volume decrease of between 12 and 15 $cm^3\ mol^{-1}$ for the high-spin to low-spin change on metMb-L,[51] but it is not clear what effects should be expected in the present case. Since the overall volume change of eq 2 is nearly zero, the net effect may not be large. Regardless of this issue, differences in the activation parameters for the k_{-1} and k_2 steps will largely cancel out given the likely scenario of early transition states in going from metMb[5] to either six-coordinate species. Thus, it follows that the reported values for $\Delta V^{\ddagger}_{on}$ mainly represent volume changes associated with the k_1 pathway. These are significantly larger than reported for the model porphyrin system.[32] This can further be seen from a comparison of the volume profiles for the metMb(H_2O) + NO and Fe(TPPS)$(H_2O)_2$ + NO reactions reported in Figure 9. Dissociation of a coordinated water molecule from an octahedral metal center is expected to be accompanied by a maximum volume increase of 13 $cm^3\ mol^{-1}$.[43] The larger value of $\Delta V^{\ddagger}_{on}$ reported here for metMb suggests that the protein may also undergo some structural rearrangement during the formation of the five-coordinate metMb.[5] The XAFS structural findings referred to above[49] indicate steric strain in the linear coordination of NO to the Fe^{III} center, which could involve an increase in the size of the protein pocket prior to the binding of NO, and therefore a larger $\Delta V^{\ddagger}_{on}$ than for the porphyrin case. In fact, the activation volume reported for the binding of NO to Fe^{III}(TPPS)$(H_2O)_2$ is identical to that recently found for water exchange on Fe^{III}(TPPS)$(H_2O)_2$,[46] suggesting that the binding of NO is controlled by the water exchange mechanism.

Microscopic reversibility argues that the reverse process will be dominated by the k_{-2} step, the dissociation of NO from the $Fe^{II}(NO^{+})$ species accompanied by a charge transfer from metal to nitrosyl to give metMb[5] plus NO and a concomitant spin change. As a result, the activation parameters must reflect the intrinsic entropy and volume changes associated with bond breakage and the solvational changes associated with solvent reorganization concurrent with charge redistribution and the spin change. Such factors are consistent with the large and positive values of $\Delta S^{\ddagger}_{off}$ and $\Delta V^{\ddagger}_{off}$ demonstrated here for metMb and previously for the water-soluble ferriheme models. The values of $\Delta V^{\ddagger}_{off}$ reported here are similar to those reported for model porphyrin complexes,[32] and the volume profiles for the metMb and model systems are shown in Figure 9. In both the heme protein and porphyrin systems, $Fe^{III}-NO$ has $Fe^{II}-NO^{+}$ character, and bond cleavage is accompanied by a formal oxidation of Fe(II) to Fe(III), which could lead to a similar volume increase in both cases. On the other hand, the more negative ΔV for the overall reaction may reflect specific solvation of the NO^{+} moiety in the case of the model compounds. Similar solvation by water is less likely in the cavity of metMb, which excludes the bulk solvent.

The "on" reactions for a variety of ferri- and ferroheme proteins and water-soluble porphyrins have been examined and demonstrate a dramatic range of reaction rates spanning 9 orders of magnitude, from $<10\ s^{-1}$ for the NO reaction of ferrous cytochrome *c*[20] to $10^9\ M^{-1}\ s^{-1}$ for the reaction of free iron(II) porphyrins with NO.[33] This range of rates is due in part to variations of the heme protein structures, particularly when the protein limits access to the metal center. For example, although the equilibrium constants for binding NO are large for ferric and ferrous cytochrome *c*, the rates are comparatively slow ($k_{on} = 7.2 \times 10^2$ and $8.3\ M^{-1}\ s^{-1}$, respectively),[20] presumably because in both cases the iron is strongly bound by both a methionine sulfur and a histidine nitrogen. However, when access is not limited by the protein, more facile reactions occur, as in the case of the reaction of NO with catalase[20] or in the present case with metmyoglobin.

Various flash photolysis studies of the analogous nitrosyl complex of ferrous myoglobin have demonstrated that the quantum yield for net photodissociation of Mb(NO) into Mb plus NO in solution is very small.[19] However, on the picosecond and femtosecond time scale it has been noted that NO is labilized but does not escape significantly from the protein, the recombination occurring much faster than dissociation of the {Mb,NO} geminate pair. On the subnanosecond time scale, the reformation of Mb(NO) does not follow a single exponential, and this observation for native Mb as well as kinetics studies of mutant forms leads to the conclusion that the heme pocket is playing a key role in the recombination pathway and that

(47) (a) Traylor, T. G.; Sharma, V. S. *Biochemistry* **1992**, *31*, 2847. (b) Wang, Y.; Averill, B. A. *J. Am. Chem. Soc.* **1996**, *118*, 3972. (c) Miller, L. S.; Pedraza, A. J.; Chance, M. R. *Biochemistry* **1997**, *36*, 12199.

(48) Enemark, J. H.; Feltham, R. D. *Coord. Chem. Rev.* **1974**, *13*, 339−406.

(49) Rich, A. M.; Armstrong, R. S.; Ellis, P. J.; Lay, P. A. *J. Am. Chem. Soc.* **1998**, *120*, 10827.

(50) Constable, E. C.; Baum, G.; Bill, E.; Dyson, R.; van Eldik, R.; Fenske, D.; Kaderli, S.; Morris, D.; Neubrand, A.; Neuburger, M.; Smith, D. R.; Wieghardt, K.; Zehnder, M.; Zuberbühler, A. D. *Chem. Eur. J.* **1999**, *5*, 498 and references therein.

(51) (a) Messana, C.; Cerdonio, M.; Shenkin, P.; Noble, R. W.; Fermi, G.; Perutz, R. N.; Perutz, M. F. *Biochemistry* **1978**, *17*, 3652. (b) Morishima, I.; Ogawa, S.; Yamada, H. *Biochemistry* **1980**, *19*, 1569.

multiple geminate-type intermediates may be invoked to explain the kinetics behavior.[14,16−17] In the present study, the bimolecular "on" reaction kinetics of the ferric complex metmyoglobin are instead shown to be dominated by the six-coordinate nature of metMb, and thus by the lability of the coordinated H_2O molecule.

These findings suggest that, although the free radical character of NO is crucial to its role as a bioregulatory molecule, this may have only a minor influence on the dynamics of the reactions with metal centers key to such biological activity. Since the odd electron in NO resides in a π^* orbital, its interaction with the metal center is unlikely to be significant, except at close distances when coordination has largely been achieved. The reaction dynamics are far more dominated by the nature of the metal center. Fast reactions require high metal center lability as in the cases of the hexacoordinate high-spin ferric porphyrin models[32] or proteins such as catalase or metmyoglobin, or an empty coordination site such as that seen for high-spin, five-coordinate ferroheme proteins or model complexes.[33] In the early stage of its reactions with such metal centers, i.e., those stages which dominate the reaction dynamics, the behavior of NO is more like that of other typical Lewis base donors. A similar conclusion was reached for oxidation reactions of different aquated metal ions and complexes of Mn(II), Fe(II), and Co(II) with a series of different free radicals such as $^{\bullet}CH_3$, $^{\bullet}O_2CH_3$, $Br_2^{\bullet-}$, and $(SCN)_2^{\bullet-}$, in which the reactions are controlled by ligand interchange processes, and the free radicals were all found to behave as "normal" nucleophiles.[52]

(52) van Eldik, R.; Cohen, H.; Meyerstein, D. *Inorg. Chem.* **1994**, *33*, 1566.

In summary, the present study provides new mechanistic information on the reaction of nitric oxide with metmyoglobin. The activation parameters $\Delta H^{\ddagger}$, $\Delta S^{\ddagger}$, and $\Delta V^{\ddagger}$ determined from the temperature and pressure dependence clearly support the ligand dissociation mechanism for the studied reaction. High-pressure measurements (both high-pressure stopped-flow and high-pressure flash photolysis studies) provide key insight into understanding the nitrosylation reaction mechanism of this ferriheme protein. Notably, the patterns of behavior for metMb are similar to that reported for water-soluble iron(III) porphyrin model systems,[32] and these systems react with NO by analogous mechanisms. Similar correlations are to be expected for other metal−ligand systems. Furthermore, the large and positive values of $\Delta V^{\ddagger}_{on}$ and $\Delta V^{\ddagger}_{off}$ point confidently to a dissociative mechanism as the common pathway and illustrate the feasibility of volume profile analyses in the assignment of detailed reaction mechanisms.

Acknowledgment. Studies at UCSB were supported by the National Science Foundation (CHE 9726889). P.C.F. is grateful for the support of the Alexander von Humboldt Foundation during aspects of these studies. Studies at UEN were supported by the Deutsche Forschungsgemeinschaft, the Fonds der Chemischen Industrie, and the Max-Buchner-Forschungsstiftung. Studies at JU were supported by the State Committee for Scientific Research, Poland, KBN (3T09A11515), and the Foundation for Polish Science ("Fastkin" No. 8/97) for the LKS.60 system. A.W. gratefully acknowledges support by DAAD.

JA001696Z